ЖЭТФ, 2014, том 146, вып. 6 (12), стр. 1210–1221

SUPERFLUID ^{3}He, A TWO-FLUID SYSTEM, WITH THE NORMAL-FLUID DYNAMICS DOMINATED BY ANDREEV REFLECTION

G. R. Pickett*

Department of Physics, Lancaster University, Lancaster, LA1 4YB, UK

Received May 26, 2014

As a specific offering towards his festschrift, we present a review the various properties of the excitation gas in superfluid ^{3}He, which depend on Andreev reflection. This phenomenon dominates many of the properties of the normal fluid, especially at the lowest temperatures. We outline the ideas behind this dominance and describe a sample of the many experiments in this system which the operation of Andreev reflection has made possible, from temperature measurement, particle detection, vortex imaging to cosmological analogues.

Contribution for the JETP special issue in honor of A. F. Andreev's 75th birthday

DOI: 10.7868/S0044451014120062

1. INTRODUCTION

This article provides a brief review of the influence of Andreev reflection on the behavior of superfluid ^{3}He. Since, as we see below, the dispersion curve of the quasiparticle/quasihole excitations depends on the relative motions of the fluid, any mechanical disturbance of the liquid gives rise to a disordered effective gap for the excitations which are no longer free to move through the liquid unconstrained. In this landscape of varying gaps, excitations are constantly being subjected to Andreev processes to the extent that the whole mechanical behavior of the normal fluid of excitations is completely dominated by such processes. This is the system where the Andreev process indeed comes into its own. However, this behavior is not a drawback. On the contrary, we are able to exploit these processes which allow us to undertake a range of experimental investigations which are otherwise experimentally inaccessible.

2. THE ANALOGY BETWEEN ANDREEV REFLECTION AT A BOUNDARY SEPARATING DIFFERENT SUPERCONDUCTORS, AND IN A REGION SEPARATING STATIONARY AND MOVING SUPERFLUID ^{3}He

The original Andreev reflection process was proposed by Aleksandr Fedorovich for describing the behavior of quasiparticles in superfluids in regions where the energy gap is changing spatially, as for example at a superconducting–normal interface or at an interface between two dissimilar superconductors with different energy gaps [1]. Of course, the unique aspect of this process is the "flavor" change made by excitations as they approach a region where the gap rises above the total energy of the excitation. In this situation an approaching excitation finds itself arriving at a minimum in the dispersion curve at which its group velocity falls to zero and then it retraces its trajectory with almost no change in its momentum but with the opposite group velocity. Thus an incoming quasiparticle is retro-reflected as a quasihole and an incoming quasihole will be reflected as a quasiparticle.

From this new understanding of the process, a whole spectrum of unique phenomena can be recognized, quasiparticle–quasihole bound states and many more. However, that is the picture we recognize from static systems to which the concept was originally applied. (The rigid metallic lattices of superconducting/normal interfaces are clearly static.)

It is the purpose of this paper to recapitulate those aspects of this behavior which we have studied in non-static contexts, i. e., in superfluids. Here the phenomenon, while operating in a similar way, has a much richer and more complex behavior. In a moving BCS system the effective energy gaps are not static but governed by the flow of the fluid adding a whole new spectrum of properties with often very counter-intuitive effects.

*E-mail: g.pickett@lancaster.ac.uk

Superfluid ^{3}He has a complex and anisotropic order parameter, but for the purposes of the present treatment we will consider only the B phase which has an energy gap in low magnetic fields with the same magnitude around the Fermi surface. Therefore, the straightforward ideas of Andreev reflection developed for simple superconductors can be transferred to superfluid ^{3}He-B directly. It is true that, while the magnitude of the B-phase gap is isotropic, the pairing is in fact anisotropic since the directional properties of the Cooper pairs vary around the Fermi sphere. However, for the arguments used here this does not really come into play until we start applying magnetic fields.

To begin, let us look at the dispersion curve of the excitations in superfluid ^{3}He (with energy gap Δ) as shown in Fig. 1A. For simplicity the curve only covers the single x-dimension and is drawn for the rest frame of the liquid. We note that there are four classes of excitations. On the right-hand side of the figure quasiparticles move in the positive x direction and quasiholes move in the $-x$ direction, both with momenta very close to the Fermi momentum value, p_F. On the left-hand side of the curve there are quasiholes moving in the x direction and quasiparticles moving in the $-x$ direction, both with momenta close to $-p_F$.

Let us assume a neighboring region of superfluid with a larger (static) gap, Δ', with the dispersion curve as shown in Fig. 1B. If we then imagine a low-energy quasiparticle from region A traveling in the x direction towards region B, then as the excitation moves into the region of increasing energy gap, it decelerates as its group velocity decreases (with the decreasing slope of the dispersion curve) and finally reaches the curve minimum, having slowed to zero velocity. It can then penetrate no further into the region of increasing gap but will retrace its trajectory with increasing velocity in the $-x$ direction, but with more or less the same total momentum as it had originally. Hence, it now has its group velocity and momentum oppositely directed and it has become a quasihole. We can use similar arguments for an incoming quasihole. This is the classical Andreev scenario.

The new aspect, which we have to take into account in the superfluid, is the fact that we can set various parts of the liquid into relative motion. Since the dispersion curve is tied to the rest frame of the liquid, then for comparing excitation energies we have to apply the correct Galilean transformation to make the various curves consistent. This reduces to the classical argument that if we observe liquid approaching us with a (small) velocity v then a fermion in that liquid approaching us with velocity w in that rest frame will appear to us to have a velocity of $v + w$ and thus the corresponding kinetic energy will be $m(v + w)^2/2$ rather than the $mw^2/2$ in its own liquid rest frame. Near the Fermi energy, the fermions have a velocity $\pm v_F$. Thus in our rest frame, we will see the energy of the dispersion curve skewed by the transformation $E' \to E + vp_F$. The curve for superfluid at rest is shown in Fig. 2A. The equivalent curve for liquid moving to the right with velocity v is shown in Fig. 2B. A quasiparticle on the right-hand side of Fig. 2A moving in the x direction could not penetrate into the moving liquid of Fig. 2B but would be Andreev-reflected and emerge traveling in the $-x$ direction but as a quasihole. Unlike in Fig. 1 the behavior of quasiparticles and quasiholes is not symmetrical. A quasihole on the left-hand side of Fig. 2A traveling in the x direction *would* be able to penetrate into the moving region. Similar arguments can be used for excitations traveling from the moving to the stationary regions.

3. THE EFFECT OF THE ANDREEV REFLECTION OF QUASIPARTICLES AND QUASIHOLES ON THE DAMPING OF A MOVING OBJECT IN SUPERFLUID ^{3}He-B

The above section concludes all the introduction to Andreev reflection in the superfluid in relative motion that we need initially to understand the basic ideas of the dynamics of the excitation gas in the superfluid. Throughout this work we assume that we are in the low-temperature limit $T \ll T_c$. Here the mean free path of the excitations is invariably much greater than any reasonable experimental dimension and we can consider the excitation motion to be entirely ballistic.

The first topic we discuss is the mechanical damping of an object moving in the superfluid, since this serves as a good introduction to the dynamics and also provides us with some important experimental tools for probing the superfluid.

Let us take again a one-dimensional toy model of a moving object where we consider the bulk liquid to be stationary but the liquid near the moving object to be at rest with respect to it. The scenario is shown in Fig. 3. The important aspect of this process is the fact that the flow field associated with the motion of the wire provides a sort of Maxwell demon which leads to different responses to the moving object from quasiparticles and quasiholes. From the figure it is apparent that quasiparticles approaching the leading side of the object will be able reach the surface but quasiholes approaching from the front cannot reach the region of liquid moving with the wire and will be Andreev-reflected,

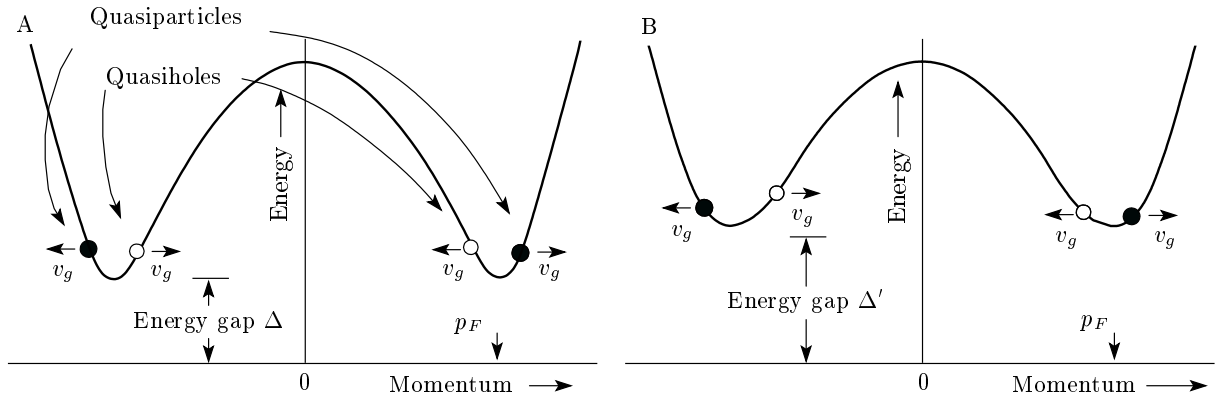

Fig. 1. The dispersion curves for two superconductors (or superfluids) with different energy gaps. A quasiparticle or quasihole in region A moving right would not be able to penetrate into the superconductor (superfluid) of region B but would undergo Andreev reflection and retrace its incoming trajectory

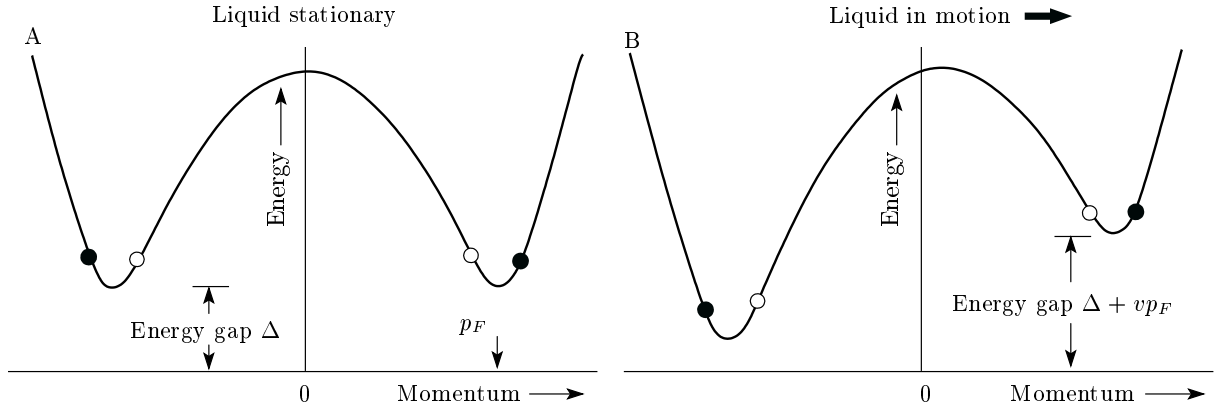

Fig. 2. A) The dispersion curve for excitations in superfluid ^{3}He-B at rest. B) The dispersion curve for the superfluid when moving with velocity v in the x direction skewed by the Galilean transformation term $E' \to E + vp_F$. A quasiparticle on the right-hand side of the curve in region A moving to the right would not be able to penetrate into the moving superfluid of region B, but would undergo Andreev reflection and retrace its incoming trajectory. Conversely, a quasihole on the left-hand side of region A moving to the right is free to enter region B

and thus cannot exchange momentum with the wire. That means that particle–hole symmetry is broken and only quasiparticles can reach the leading boundary of the object to be normally reflected transferring the momentum of $2p_F$ to the object, and thereby damping the motion. Conversely on the trailing side, quasiparticles cannot reach the object and only quasiholes can reach the surface to be normally reflected but also transferring $2p_F$ of momentum to the object and also damping the motion. In other words, the quasiparticles hitting the front side of the object slow it down, but also the quasiholes hitting the rear side slow it down. This has the effect of providing an enormous damping force on the moving object. The energies of the excitations are very low in the ballistic regime and have a vanishing density being well below the superfluid transition temperature but each collision exchanges a momentum of the order of the Fermi momentum which is very large. In short, the damping force on a moving object is orders of magnitude greater than it would be for a classical gas of particles with the same effective mass, density, and temperature.

Using this simple one-dimensional picture, and assuming that the moving object presents an area a normal to the motion, we can find the damping force by simply integrating over those excitations which can reach the surface of the object and exchange $2p_F$, using the arguments of Ref. [1]. The integral takes the form (with the usual notation)

$$F = -\int_{\Delta}^{\Delta + p_F v} 8p_F a g(E) \exp\left(-\frac{E}{kT}\right) v_g \, dE.$$

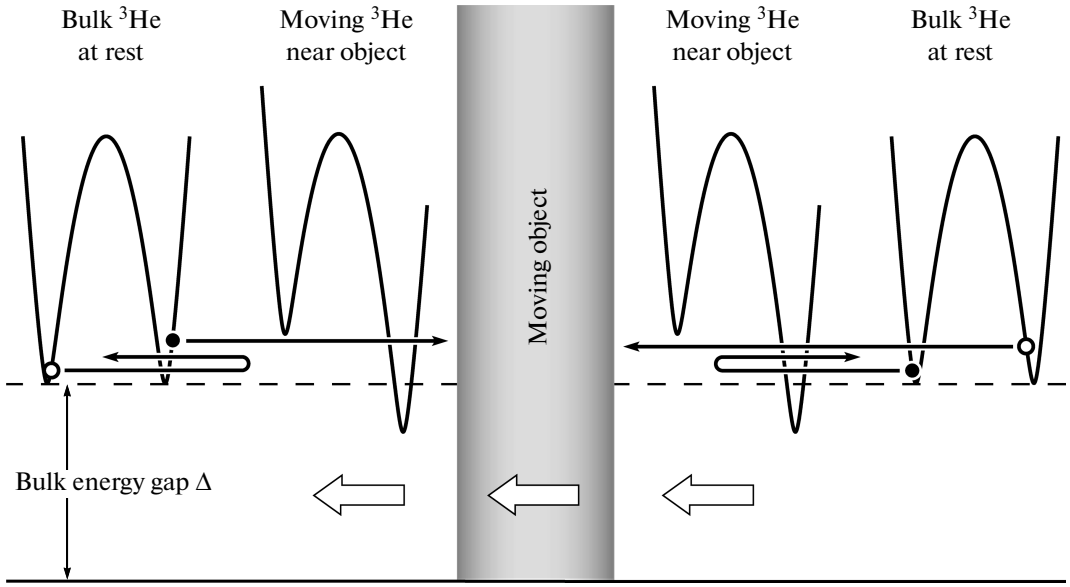

Fig. 3. The excitation dispersion curves for excitations for regions of the liquid near a moving object in the superfluid. Quasiparticles approaching the object from the leading side can reach the surface and be normally reflected, whereas quasiholes approaching from the same side cannot. The inverse occurs for excitations approaching from the rear of the object (see text)

Since the group velocity v_g is $\partial E/\partial p$ and the density of states is $g(E) = (2/h)\partial p/\partial E$ a convenient cancellation occurs and the integral reduces to

$$F = -\int_{\Delta}^{\Delta + p_F v} \frac{16 a p_F}{h} \exp\left(-\frac{E}{kT}\right) dE.$$

This yields

$$F = \frac{16 a p_F kT}{h} \exp\left(-\frac{\Delta}{kT}\right)\left[1 - \exp\left(-\frac{p_F v}{kT}\right)\right],$$

which gives a force of the form

$$F = v\frac{16 a p_F^2}{h} \exp\left(-\frac{\Delta}{kT}\right)$$

in the low-velocity limit, where $p_F v \ll kT$.

This force is very nonlinear in v. However, at low velocities when $p_F v \ll kT$ the damping becomes linear in v and proportional to the gap Boltzmann factor $\exp(-\Delta/kT)$ [2]. Since the latter is a very rapidly changing function of temperature, the damping on a moving object in superfluid ^{3}He-B provides an incredibly sensitive thermometer measuring the temperature of the liquid directly. It is at first sight paradoxical that we can determine the temperature of a superfluid by measuring the mechanical damping effect of the normal fluid, despite the fact that the normal fluid density is vanishingly small. This all arises from the Andreev-reflection Maxwell demon completely overwhelming particle–hole symmetry.

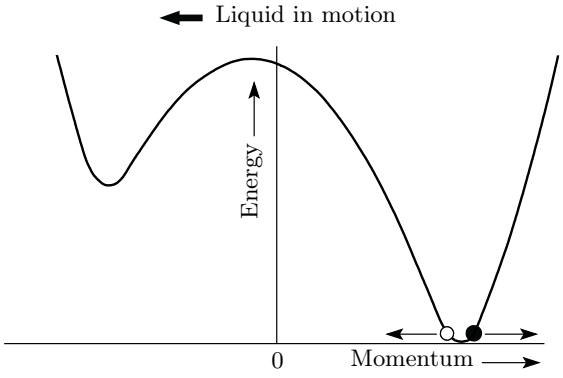

Fig. 4. The Landau critical velocity condition, when the velocity of the moving liquid becomes large enough that one minimum in the dispersion curve falls to zero energy (and therefore excitations at this point on the dispersion curve can be freely created by the object), see text

This serendipitous behavior immediately allows us to make many different types of measurement in the superfluid in the "pure" quantum regime ($\rho_n \sim 0$) because we have a *very* sensitive thermometer in the liquid.

At this point we should note that if a moving body in the liquid is traveling fast enough that $v = p_F/\Delta$, then one minimum in the dispersion curve in the rest

frame of the moving object decreases to zero energy, as shown in Fig. 4. At this velocity, in the frame of the moving body, the energy of quasiparticle and quasihole excitations at the minimum becomes zero. This means that a moving body which scatters excitations elastically in its own rest frame can thus freely create excitations at the dispersion curve minimum as their energies are zero. This is the Landau critical velocity where the superfluidity breaks down and Cooper pairs in the fluid are broken by the motion. As seen in the Fig. 4, at this critical velocity quasiparticles are then emitted in the direction of motion of the scattering body and quasiholes are emitted in the reverse direction.

Therefore, a moving object can detect quasiparticle and quasihole excitations from their contribution to the damping of the motion but, furthermore, when the object moves fast enough it can also create these excitations thus becoming an excitation source. The importance of this, as we shall see later, is that we now have the basic elements for producing an excitation spectrometer: a potential source and a potential detector.

4. VIBRATING WIRE RESONATORS AND QUARTZ "TUNING-FORK" RESONATORS

To measure the drag on a moving object in practice, we have used the vibrating wire resonator as shown in Fig. 5. This consists of a thin superconducting wire bowed into an approximate semicircle of a few mm across. We normally begin with filamentary superconducting wire and over the active region etch off the outer metallic matrix and cut the exposed filaments, leaving just a single strand. It is possible, with care, to make resonators with filaments down to micron diameters in this way. Such a device has a mechanical resonance moving normal to the semicircle plane of from 100 to 1000 Hz depending on the wire used. To detect the very small damping at the lowest temperatures, the wires need to be of the smallest diameter possible to make the inertia of the wire small in comparison to the damping. A vertical magnetic field is applied and the wire's mechanical resonance is excited from the Lorentz force on a resonant current applied to the loop. If the wire is superconducting there is no resistive voltage developed across the wire and thus a measure of the oscillating voltage across the wire gives a direct measure of the velocity. The frequency can then be scanned across the mechanical resonance and the damping (width at half height) measured.

The damping measured in this way for a rather thicker wire (diameter about 0.125 mm) is shown in

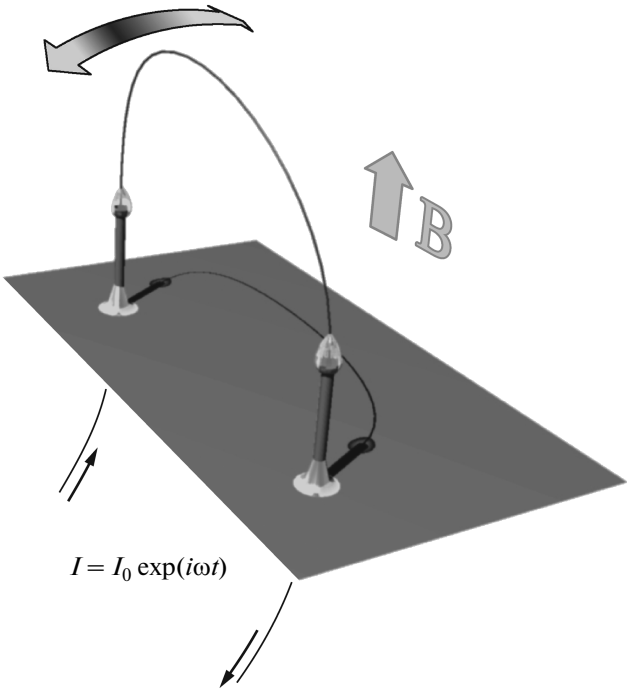

Fig. 5. A vibrating wire resonator

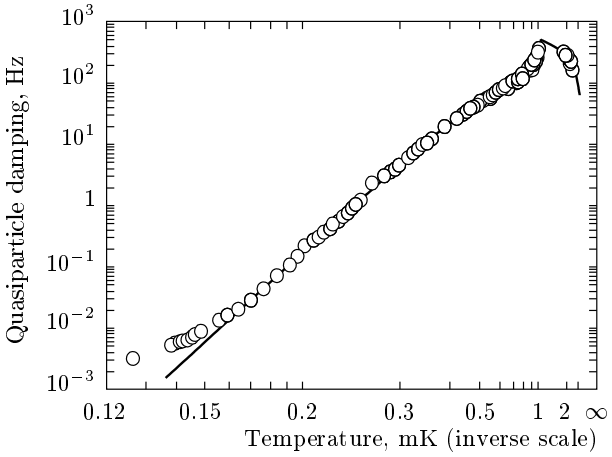

Fig. 6. The damping of a vibrating wire resonator (the width of the Lorentzian line shape at half height) in superfluid ^{3}He-B at zero pressure plotted against the temperature as measured by a platinum NMR thermometer [3]. Note that below about 0.3 mK where the system enters the ballistic limit (i. e., where the mean free paths of the excitations exceeds the diameter of the wire) the damping follows the gap Boltzmann factor $\exp(-\Delta/kT)$. The deviation at low temperature occurs when the liquid damping becomes so low that we begin to see the small internal damping of the wire material itself

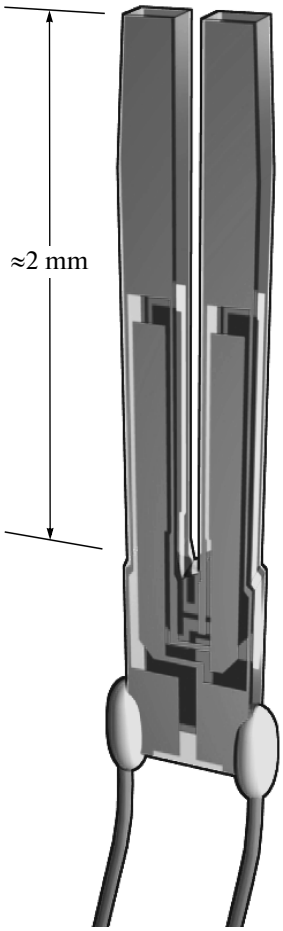

Fig. 7. A quartz tuning-fork resonator. The active region near the tips of the arms is only a fraction of a millimetre in size

Fig. 6 [3]. The simple treatment above only applies in the ballistic limit where the excitation mean free paths are large compared to the wire dimension (cross-section diameter). For the wire used for this data, this occurs below 0.3 mK. Below this we see that the damping closely follows the gap Boltzmann factor $\exp(-\Delta/kT)$. At the lowest temperatures we start seeing deviations from the effect of the nuisance damping of the wire itself. Thinner wires of a few microns in diameter can be followed to much lower temperatures.

The attraction of such resonators is that the geometry is simple and the wire can be approximated to a straight cylinder moving in the superfluid and is amenable to simulation. Unfortunately these devices turn out to be too large for our current needs (as discussed below) and we have moved to using simple quartz tuning-fork resonators, as shown in Fig. 7. These have much smaller active regions and are readily available (and producible). The geometry is much more complicated but the response turns out to be essentially similar to that of the vibrating wires [4]. The disadvantage of the relatively large mass of the moving legs of the resonator is compensated by the more accurate measurement which comes with the much higher frequency of the mechanical resonance.

5. MAKING A BOLOMETER: THE QUASIPARTICLE BLACK-BODY RADIATOR

Before we discuss some of the more sophisticated experiments which we have made by exploiting the Andreev reflection properties of the superfluid, we need to introduce one more device, the quasiparticle black-body radiator, developed by Shaun Fisher while a graduate student [5]. This is precisely what it says, a classic black-body radiator, but one for quasiparticles rather than photons. It consists of a small container (of dimensions a few mm) containing two vibrating wire resonators. One measures the excitation density inside the container (as described above), in other words the temperature, and the second can be excited above the Landau critical velocity to break Cooper pairs to create a quasiparticle gas. This vibrating wire resonator is thus a heater, but one which heats the liquid directly. When this vibrating wire resonator is pair breaking, the damping on the wire clearly increases which we can measure electrically and thus calibrate what power is being generated in the liquid in the box. The box has a small orifice leading to the outside and is immersed in bulk superfluid. The device has two modes. The heater wire resonator can be excited thereby creating a thermal beam of excitations (of known power and temperature) leaving the box by the orifice. This we can think of as "generator" mode. We can also use the device passively to measure energy deposited inside the box from the increase in the temperature inside. This is "detector" mode. Such a black-body radiator is shown in Fig. 8.

In detector mode the energy sensitivity of these devices is remarkable. A typical calibration is shown in Fig. 9, where we see that the response is linear over many orders of magnitude and the sensitivity approaches the femtowatt level. These devices make very good low-energy particle detectors [6].

This is the final tool we need to make a whole range of experiments in superfluid ^{3}He. The first we shall describe (only qualitatively) is the most direct measurement of Andreev reflection which we known of [7]. It illustrates a number of characteristics of Andreev re-

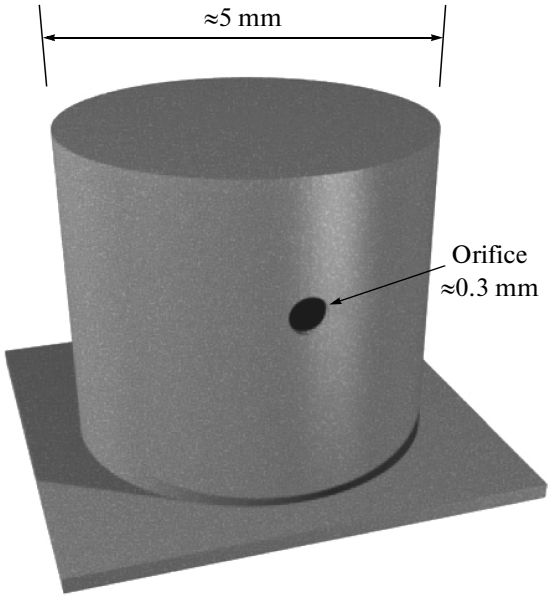

Fig. 8. A black-body radiator. This is a small container filled with superfluid ^{3}He immersed in the bulk superfluid and connected to it via the small orifice. Inside the container are two vibrating wire resonators, one to measure the excitation density (the temperature) and the other to heat the superfluid by pair breaking

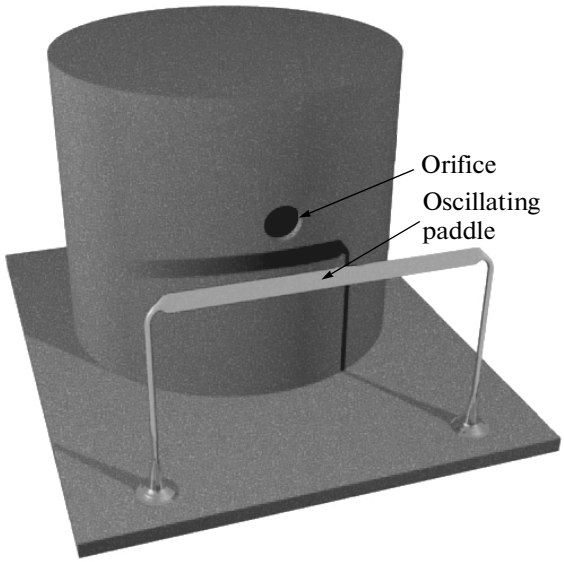

Fig. 10. A black-body radiator with a moving paddle placed in front of the orifice. When the paddle is in motion, the velocity gradient of the associated flow field causes the Andreev reflection of a fraction of the excitations in the emitted beam, reflecting them back into the box because of the retro-reflection properties of the process (see text)

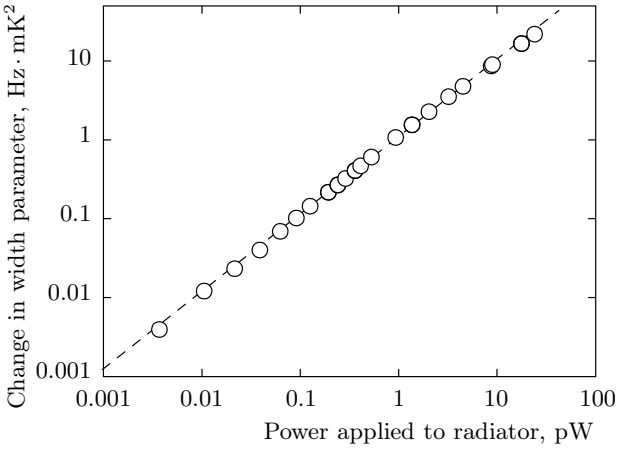

Fig. 9. The power sensitivity of a typical black-body radiator

flection which we exploit in the measurement. We use a black-body radiator as shown in Fig. 8 but with a moving paddle placed in front of the radiator orifice. This is shown in Fig. 10.

The box is operated in generator mode with the heater wire inside producing a beam of excitations which is emitted through the orifice into the bulk surrounding superfluid. The excitations scatter off the paddle and other boundaries and are spread throughout the bulk surrounding liquid. At equilibrium this gives rise to an elevated temperature inside the radiator such that the energy emitted from the box in the beam just balances the heating applied to the heater wire. The flat paddle in front of the orifice is in fact a slightly deformed vibrating wire resonator and can be set in motion in the same way. To make the demonstration we now oscillate the paddle. This means that the flat paddle surface is moving backward and forward in the emitted beam of quasiparticles and quasiholes. Something remarkable now happens. When the paddle was stationary, excitations in the beam hitting the paddle surface were normally scattered and spread all over the bulk liquid. As soon as the paddle is moving, half the excitations are Andreev-reflected by the moving boundary layer of liquid. (This happens in exactly the same way as the reflection of excitations from a moving wire as shown in Fig. 3.)

The great difference is that now when we have Andreev rather than normal reflection, the scattered excitations are accurately retro-reflected and retrace their trajectories, and are returned into the radiator box. This accurate retro-reflection aspect of Andreev reflec-

tion we exploit in several experiments. In this case, the Andreev reflection leads to a large fraction of the emitted excitations being returned into the radiator and thus the excitation density/temperature inside the radiator increases further. This is a new mechano-caloric effect in that as soon as Andreev reflection is introduced into the scenario, the temperature in the box depends on the distribution of liquid velocities out in the bulk liquid remote from the box. This is the best demonstration of the retro-reflection aspect of Andreev reflection of which we are aware.

6. USING ANDREEV REFLECTION TO VISUALIZE VORTICES

Not only are moving objects in the superfluid associated with flow fields. Mass vortices in the superfluid also carry their own circulation. The Andreev reflection of excitation beams by vortices in superfluid ^{3}He-B gives us a most powerful tool for visualising the vortex distribution in the superfluid. If we imagine placing a vortex in a beam of quasiparticle/quasihole excitations, the flow fields around the vortex core will Andreev reflect excitations in a similar way to that caused by the backflow around a moving object. The scenario is illustrated in Fig. 11. Since there is in any case a flow round a vortex we can picture the situation as that in Fig. 3 except that the vortex provides the local motion so we can therefore just leave out the wire. Thus on one side of the vortex the picture will be that of Fig. 3 and on the other side, it will be similar but with the local velocity reversed. In other words, since the flow is in the opposite direction on the two opposite sides of the vortex, quasiparticles and quasiholes are differently Andreev-reflected on the two sides, but the net effect is that a large fraction of the excitations is retro-reflected. This means that a vortex tangle throws shadows when illuminated by a beam of excitations. Since the flow fields extend a considerable way out from the vortex cores this "optical" obstacle is significantly large and allows us to visualize a tangle of vortices, for which we have almost no other experimental tools. The detection can be done by observing the transmitted part of the beam, or by observing that part of the beam retro-reflected.

But first we need some vortices to image. Very happily for us, a vibrating wire resonator can also be used to create vortices, probably by exciting existing vortex loops pinned to the wire surface, but the precise mechanism is not completely understood. However, when the moving wire reaches the critical velocity it starts breaking pairs by the Landau process but a small fraction of the dissipated energy (say, one part in 10^3) goes into creating vortices [8]. Thus, by running a vibrating wire resonator above its critical velocity, we are able to create a tangle of vorticity at will.

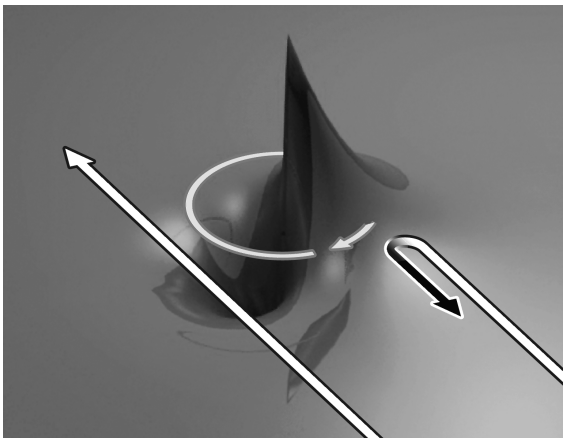

Fig. 11. The effective "potential" presented by a vortex flow field to quasihole excitations moving as shown. On one side of the vortex, quasiholes are Andreev-reflected while on the other side they can travel through the flow field freely. The converse applies to quasiparticles. The extent of the vortex flow field which is capable of doing this is of macroscopic size and thus a tangle of vortices throws very significant "shadows" when illuminated by a quasiparticle/quasihole beam

The first experiment we discuss is one where we observe such a tangle of vortices by the Andreev-reflected component of an illuminating beam [9]. We use the more or less identical setup to that shown in Fig. 10 above except that here we replace the moving paddle by the flow field of a tangle of vorticity created by a vibrating wire resonator. The experimental setup is shown in Fig. 12. In Fig. 12*a* we see a schematic of the black-body radiator containing the thermometer and heater wires. The radiator is emitting a beam of excitations which are incident on a stationary vibrating wire resonator in front of the orifice. No Andreev reflection takes place and the emitted beam is dispersed into the bulk superfluid. In Fig. 12*b* we have excited the vibrating wire resonator to create a vortex tangle, which is Andreev-reflecting a fraction of the beam back into the box, thereby raising the excitation density inside and allowing us to calculate the fraction reflected.

A typical result is shown in Fig. 13. Here we show the fraction of the beam reflected as a function of the maximum velocity of the vortex-creating vibrating wire resonator in front of the orifice. We see that there is no reflection before the critical velocity for vortex cre-

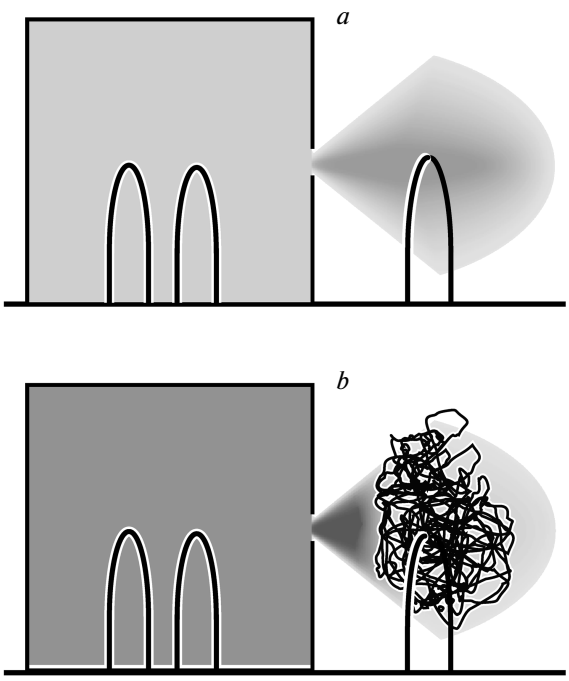

Fig. 12. A schematic picture of the experiment to detect the density of a tangle of vortices in superfluid ^{3}He. A vibrating wire resonator is placed in the beam of excitations emitted by a black-body radiator. When the vibrating wire resonator is excited to high enough velocity to create a vortex tangle, the flow fields associated with the vortices retro-reflect a fraction of the excitations back into the radiator allowing us to calculate the vortex line density in the tangle

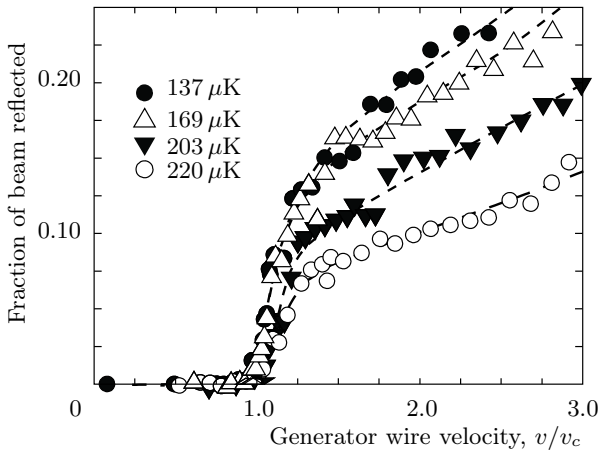

Fig. 13. The fraction of the beam reflected back into the radiator box as shown in Fig. 12 as a function of the velocity of the vibrating wire resonator in front of the orifice. When the vibrating wire resonator reaches the critical velocity for the creation of vorticity (v_c in the figure), the vorticity produced then begins to reflect excitations back into the container, raising its temperature (see text)

ation (v_c) is reached. At this point the Andreev process starts and more and more of the beam is reflected back into the box as the vorticity level increases. We can readily calculate the cross section for reflection for a vortex line and knowing the rough size of the tangle (a few millimetres across) we can deduce the vortex line density. At the lowest levels of vorticity which we can detect near v_c the vortex spacing is of the order of 0.1 mm. That is a very tenuous tangle if only a few millimetres across. That means we should be able to detect individual vortices if we choose the correct geometry.

7. USING SUPERFLUID ^{3}He TO SIMULATE BRANE ANNIHILATION: TABLETOP COSMOLOGY

Our exploitation of Andreev reflection in the superfluid can take us in many directions. In the following case it takes us into cosmology [10]. The internal structure of the ^{3}He condensate is very similar to that of the Universe. At the superfluid transition, in the most general formulation, the condensate has to choose a phase ϕ, in other words, an angle or direction in 2-space. In symmetry terms this means breaking $U(1)$ symmetry. Since the Cooper pairs have both a nuclear spin of 1 and an orbital angular momentum of 1, the two momenta each have to choose a direction in 3-space, equivalent to breaking $SO(3)$ symmetry. Thus the total symmetries broken in forming the superfluid state are $SO(3)^L \times SO(3)^S \times U(1)$, the first two factors representing the orientations of the orbital and spin directions. It is believed that the Universe underwent several transitions soon after the Big Bang which resulted in the differentiation of the strong force first and then the separation of the weak and electromagnetic forces, resulting in the breaking of the symmetries $SU(3) \times SU(2) \times U(1)$. These are clearly not equivalent to those in the superfluid, but they are similar enough that there has been much interest over the last two decades in examining cosmological analogies in superfluid ^{3}He.

One analogy to which we have drawn attention in this context is the possibility of using the phase interface between the two phases of ^{3}He, the A phase and the B phase, as a model for a cosmological brane. The two common phases of ^{3}He can exist down to zero

temperature in the appropriate magnetic fields. At the lowest temperatures, where the normal fluid fraction is negligible, both phases are made up of a coherent condensate (the superfluid fraction) with only a vanishing number of excitations above this "vacuum" (the normal fluid fraction). If we apply a magnetic field gradient to the superfluid which is large enough at the high end to stabilize the A phase at approximately zero temperature, then we can create an A–B phase boundary between the two phases, B in the low-field region and A in the high-field region. Since this is a 2D boundary between two coherent condensates, it is itself a coherent 2D object. Its internal structure is not simple as the order parameter has to undergo a complex pirouette to transit smoothly from the A-phase symmetry to the B-phase symmetry. Nevertheless this is perhaps the most coherent 2D structure to which we currently have experimental access, and it is this structure which will serve as our analogue cosmological brane.

To understand the significance of that, in brief, it is possible that our Universe is a 3D brane embedded in a surrounding 4D (or higher) matrix. Such a possibility can solve a number of problems concerned with theories which require many dimensions, while we are only sensitive to three. It has also been suggested that brane collisions and annihilations in the early Universe may have triggered or brought to an end epochs of inflation. One consequence is the possibility that such an annihilation can leave topological defects in the structure of space–time. These structures are protected topologically and thus may survive until our current era. That is all easy to say, but since such events are so remote from us, both in time and in intuition, any simulation of the process can only help by assisting the insight of those working in the field.

Without going into details, with a profiled magnetic field we can stabilize a thin slice of A phase in a matrix of B phase. The slice is bounded by an A–B interface and a B–A interface. These are our two branes (or brane and antibrane). If we suddenly reduce the field, the slice of A phase will vanish with the "annihilation" of the two "branes". We then look for defects in our metric which is the "texture" of the superfluid which describes the map of the directions of the S- and L-vectors in the coherent condensate. If, after annihilating the two branes together, we are left with topological defects in the texture, then we should be able to detect them. A schematic of the experiment is shown in Fig. 14.

We confine the superfluid in a cylinder and measure the impedance of the column to the flow of quasiparticle/quasihole excitations along the axis. We run a heater wire at the bottom of the cell to provide a source of excitations and by measuring the excitation density at the top and bottom of the column we can determine the excitation gradient along the axis and thus the excitation flux. We then apply the profiled field to create the A-phase slab in the middle of the cell.

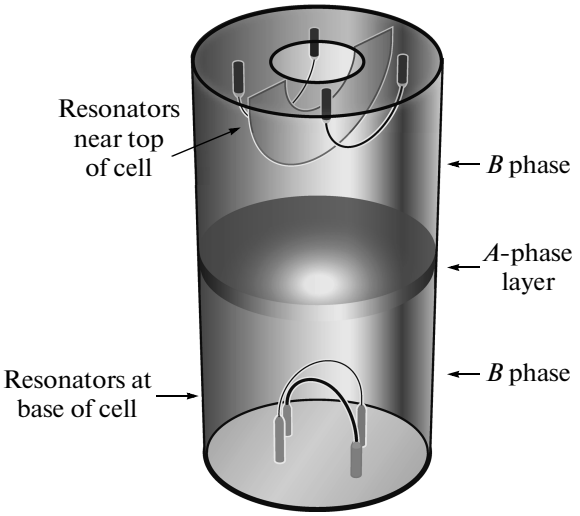

Fig. 14. The experimental arrangement used to investigate "brane" annihilation. We measure the impedance to an excitation flow of a column of superfluid ^{3}He before and after we "annihilate" a thin layer of A-phase liquid

The one extra piece of information we need to know is that in the B phase an applied magnetic field distorts the energy gap which is no longer isotropic but flattened along the direction of the L-vector. Thus if the normally smooth texture is disturbed by defects, then in a magnetic field the confused directions of the L-vector associated with the defect cause a rough mountain terrain of effective energy gaps and excitations will have difficulty penetrating but will be reflected or localized by Andreev processes.

To make the measurement we raise the field to just below that necessary to stabilise the A-phase layer and measure the impedance of the column of superfluid to the flow of excitations. We then increase the field by just the small amount needed to create the A-phase layer. If we measure the impedance again, we will find it larger because of the extra barrier presented by the two phase boundaries which cross the column. However, the important part comes next. We suddenly drop the field just enough to lose the A-phase layer, that is, back to the starting value, and look at the impedance

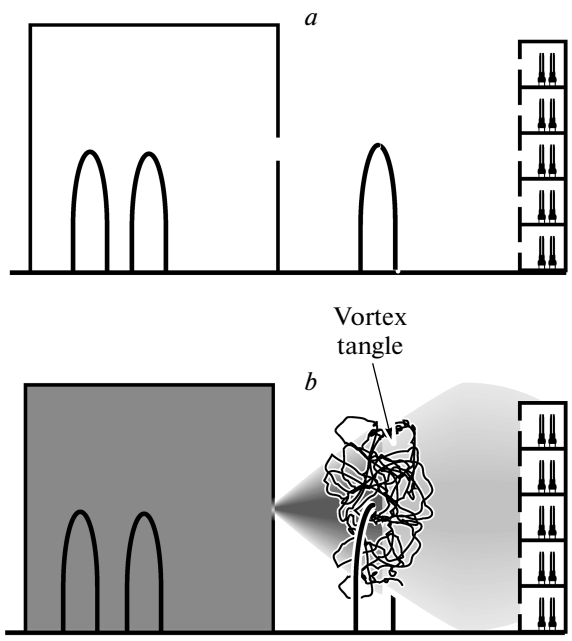

Fig. 15. The vortex video camera. The arrangement is similar to that of Fig. 12. We have a black-body radiator emitting an excitation beam into a region where we can generate a vortex tangle with a vibrating wire. However in this case we detect the transmitted rather than reflected beam, by a 5×5 array of mini black-body radiator detectors

again. If the impedance is the same as that we started with, then nothing has happened, but if it is higher, then we are seeing the added effect of defects generated by the annihilation. In the event we see a fairly large difference. Thus we do see that defects are produced and we are now working to identify what geometrical form these defects have. In any case, we have provided some ideas for the cosmologists to think about (and fortunately we did not trigger any further inflation).

8. A VORTEX VIDEO CAMERA OPERATING AT ABOUT 100 μK?

Finally, returning to our experience of imaging vortices as described in Sec. 6, we noted then that at low vortex densities, we are sensitive to individual vortices. The "camera" described in Sec. 6 is not very impressive as it only has essentially a single pixel. However, by using quartz tuning-fork resonators which are small enough, we have been able to make a 5×5 array of black-body detectors which provide a coarse-resolution video camera to image the evolution of a vortex tangle in real time and in space. The dynamics of vortices are of considerable current interest but our means to interact with them are limited and a video of this form would be very valuable. A schematic of the experiment is shown in Fig. 15. The arrangement is an extension and conceptually very similar to that of Fig. 12. We have a black-body radiator which acts as a source. Facing the beam orifice, we have a vibrating wire resonator to generate the vorticity which we will image. Then we have the 5×5 array of mini black-body radiators which then detect those parts of the beam which have not been reflected by the vortices in the tangle. We recall that this whole device is predicated on the fact that the Andreev process will remove a large fraction of the excitations from the beam to throw the shadows which we detect.

This is a video camera working at about 100 μK in superfluid ^{3}He. At present we have such a device running and we are trying to understand how to interpret the data produced. Nevertheless it does operate as envisaged and is another illustration of how dominant Andreev reflection is in this system.

It is a pleasure to write this short review of the influence of Andreev reflection on the properties of superfluid ^{3}He and the wide range of experiments which these processes allow us to make. We are very conscious that without the contribution of Aleksandr Fedorovich in formulating the original ideas we would not have been able to achieve a fraction of what we have managed to do in this field.

We are happy to acknowledge that the work described above is the result of the many combined efforts of the many members of the Lancaster microkelvin group, too numerous to list here individually, but without which this work would not have been possible.

REFERENCES

1. A. F. Andreev, Zh. Eksp. Teor. Fiz. **46**, 1823 (1964) [Sov. Phys. JETP **19**, 1228 (1964)].

2. S. N. Fisher, A. M. Guénault, C. J. Kennedy, and G. R. Pickett, Phys. Rev. Lett. **64**, 2566 (1989).

3. A. M. Guénault, V. Keith, C. J. Kennedy, S. G. Mussett, and G. R. Pickett, J. Low Temp. Phys. **62**, 511 (1986).

4. D. I. Bradley, P. Crookston, S. N. Fisher, A. Ganshin, A. M. Guénault, R. P. Haley, M. J. Jackson, G. R. Pickett, R. Schanen, and V. Tsepelin, J. Low Temp. Phys. **157**, 476 (2009).

5. S. N. Fisher, A. M. Guénault, C. J. Kennedy, and G. R. Pickett, Phys. Rev. Lett. **69**, 1073 (1992).

6. D. I. Bradley, Yu. M. Bunkov, D. J. Cousins, M. P. Enrico, S. N. Fisher, M. R. Follows, A. M. Guénault, W. M. Hayes, G. R. Pickett, and T. Sloan, Phys. Rev. Lett. **75**, 1887 (1995).

7. M. P. Enrico, S. N. Fisher, A. M. Guénault, G. R. Pickett, and K. Torizuka, Phys. Rev. Lett. **70**, 1846 (1993).

8. S. N. Fisher, A. J. Hale, A. M. Guénault, and G. R. Pickett, Phys. Rev. Lett. **86**, 244 (2001).

9. D. I. Bradley, S. N. Fisher, A. M. Guénault, M. R. Lowe, G. R. Pickett, A. Rahm, and R. C. V. Whitehead, Phys. Rev. Lett. **93**, 235302 (2004).

10. D. I. Bradley, S. N. Fisher, A. M. Guénault, R. P. Haley, J. Kopu, H. Martin, G. R. Pickett, J. E. Roberts, and V. Tsepelin, Nature Phys. **4**, 46 (2008).